Naval Research Laboratory

Washington, DC 20375-5320

NRL/MR/6440--96-7839

Magnetic Fluxtube Tunneling

RUSSELL B. DAHLBURG

Laboratory for Computational Physics & Fluid Dynamics
Center for Computational Physics Development

SPIRO K. ANTIOCHOS

E.O. Hulburt Center For Space Research
Solar Terrestrial Relationships Branch

D. NORTON

SAIC
Monterey, CA

April 3, 1996

REPORT DOCUMENTATION PAGE			Form Approved OMB No. 0704-0188

1. AGENCY USE ONLY (*Leave Blank*)	2. REPORT DATE	3. REPORT TYPE AND DATES COVERED
	April 3, 1996	

4. TITLE AND SUBTITLE	5. FUNDING NUMBERS
Magnetic Fluxtube Tunneling	NASA
6. AUTHOR(S) Russell B. Dahlburg, Spiro K. Antiochos* and D. Norton**	
7. PERFORMING ORGANIZATION NAME(S) AND ADDRESS(ES) Naval Research Laboratory Washington, DC 20375-5344	8. PERFORMING ORGANIZATION REPORT NUMBER NRL/MR/6440--96-7839
9. SPONSORING/MONITORING AGENCY NAME(S) AND ADDRESS(ES) National Aeronautics and Space Administration Washington, DC 20546	10. SPONSORING/MONITORING AGENCY REPORT NUMBER

11. SUPPLEMENTARY NOTES

*E.O. Hulburt Center for Space Research/Solar Terrestrial Relationships Branch
**SAIC, 550 Camino el Estero, Suite 205, Monterey, CA 93943

12a. DISTRIBUTION/AVAILABILITY STATEMENT	12b. DISTRIBUTION CODE
Approved for public release; distribution unlimited.	

13. ABSTRACT (*Maximum 200 words*)

We present numerical simulations of the collision and subsequent interaction of two initially orthogonal, twisted, force-free field magnetic fluxtubes. The simulations were carried out using a new three-dimensional explicit parallelized Fourier collocation algorithm for solving the viscoresistive equations of compressible magnetohydrodynamics. It is found that, under a wide range of conditions, the fluxtubes can "tunnel" through each other. Two key conditions must be satisfied for tunneling to occur: the magnetic field must be highly twisted with a field line pitch $>>1$, and the magnetic Lundquist number must be somewhat large, ≥ 2880. this tunneling behavior has not been seen previously in studies of either vortex tube or magnetic fluxtube interactions. An examination of magnetic field lines shows that tunneling is due to a double-reconnection mechanism. Initially orthogonal field lines reconnect at two specific locations, exchange interacting sections and "pass" through each other. The implications of these results for solar and space plasmas are discussed.

14. SUBJECT TERMS		15. NUMBER OF PAGES
Magnetic fluxtubes Magnetic reconnection High performance computing	Numerical simulation	17
		16. PRICE CODE

17. SECURITY CLASSIFICATION OF REPORT	18. SECURITY CLASSIFICATION OF THIS PAGE	19. SECURITY CLASSIFICATION OF ABSTRACT	20. LIMITATION OF ABSTRACT
UNCLASSIFIED	UNCLASSIFIED	UNCLASSIFIED	UL

NSN 7540-01-280-5500

Standard Form 298 (Rev. 2-89)
Prescribed by ANSI Std 239-18
298-102

MAGNETIC FLUXTUBE TUNNELING

Introduction

Models of magnetic reconnection in the Sun's interior and atmosphere usually begin with a purely two-dimensional geometry. However, the magnetic field at the solar photosphere is observed to be organized into isolated flux bundles [1], a structure which must continue into the corona. In addition, photospheric motions "wind up" this magnetic field, producing twisted fluxtubes [2] [3]. Interaction between fluxtubes has been proposed as a mechanism for coronal heating [4] [5] [6] and might be the origin of the fine-scale temporal variability of hard X-ray and microwave emission observed in two-ribbon flares [7] [8]. Fluxtubes are widely believed to be the dominant magnetic structure in the convection zone, [9] Coronal mass ejections have been identified in the interplanetary medium as flux ropes, [10] which are thought to be essential ingredients for reconnection at the magnetopause [11] and magnetotail [12]. Therefore, a key issue for understanding many important phenomena in solar and space physics is the nature of fluxtube interaction.

We are using numerical simulations to investigate the basic physics of magnetic fluxtube collision and reconnection. Our explicit, Fourier collocation algorithm, which is described in detail elsewhere [13] [14], solves the three-dimensional, compressible, dissipative magnetofluid equations in a dimensionless form[14]. The geometry used is that of a triply periodic cube with sides equal to 2π, making a Fourier spectral method the optimal choice for spatial discretization. The results described here were computed by a parallelized version of our code recently implemented on the 256 processor NRL TMC CM5E [15]. A typical resolution for the runs in this paper is 128^3 Fourier modes, requiring approximately 5 s per timestep and 1.05 GB of parallel memory.

Manuscript approved February 26, 1996.

The initial conditions consist of two orthogonal fluxtubes and a flow field which drives them together. Each of the tubes is initialized using the Gold-Hoyle model of a uniformly twisted, cylindrical, force-free magnetic field ($\mathbf{B} = (B_x, B_y, B_z)$) [16] , *viz.*,

$$B_x = -\frac{B_0 br \sin\phi}{1+b^2r^2}; \quad B_y = \frac{B_0 br \cos\phi}{1+b^2r^2}; \quad B_z = \frac{B_0}{1+b^2r^2}, \tag{1}$$

where $B_0 = 4$, and r and ϕ are the radial and cylindrical coordinates of the fluxtube. The parameter b measures the field line pitch *i.e.*, $b = d\phi/dz$. In order to maintain ideal equilibrium, the uniform gas pressure (p) outside the tube is set to $p = p_0 + 2B_0^2/(1+b^2R^2)$, where $p_0 = 20/3$ is the gas pressure inside the tube, and $R = 11\pi/48$ is the fluxtube radius. To ameliorate the Gibbs phenomenon due to the Fourier series discretization of the sharp cutoff at $r = R$, we pass these initial conditions through a raised cosine filter [17]. The initial density is uniform, $\rho = 1$. These values for B_0 and p_0 yield a plasma $\beta = 0.42$ at the fluxtube axis. We center one tube at $(x = 5\pi/4, z = \pi)$. A second tube, rotated by $\pi/2$, is centered at $(x = 3\pi/4, y = 3\pi/4)$ to break the symmetry. There are four physically distinct relative orientations for the fluxtubes, depending on the choice of the axial and azimuthal magnetic field in each of the tubes. In all our simulations the twist and orientation are chosen so as to maximize the possibility of reconnection — where they collide, the axial (azimuthal) field of the horizontal tube in the collision region is directed opposite to the azimuthal (axial) field of the vertical tube, as shown in Figure 1.

The two fluxtubes are driven together by an initial velocity field given by:

$$\mathbf{v}(x, y, z, t=0) = \epsilon_v \Big[-\sin x(\cos y + \cos z)\hat{\mathbf{e}}_x + \cos x(\sin y\hat{\mathbf{e}}_y + \sin z\hat{\mathbf{e}}_z) \Big] \tag{2}$$

The velocity amplitude is chosen to be 2.5% of the Alfvén speed at tube center, $\epsilon_v = 0.1$, which is equivalent to 4.25% of the sound speed outside the tubes. It should be emphasized that we do not impose any subsequent driver on the system, so that the fluxtubes evolve freely. Uniform and isotropic viscosity and resistivity are used, and are chosen so that the resistive and viscous Lundquist numbers are equal. The two parameters that are varied in our system are the field line pitch or twist, b, and the Lundquist number, S. Low and high twist ($b = 1$ and 10), and low and high Lundquist number ($S = 576$ and 2880) runs have been performed.

Results

In all cases we find that the fluxtubes collide and begin to reconnect as a result of their initial velocity. The standard picture for this process is that the magnetic field of one tube opposes the motion of the other tube. A thin current layer builds up between the two tubes, and if the magnetofluid is resistive and the orientation of the field lines favorable, reconnection occurs at the Petschek rate [18], the Sweet-Parker rate [9], or the linear tearing rate [7]. The reconnected field lines will then pull away from the reconnection site: this is the basis of particle acceleration by the "slingshot effect" [19]. The expectation is that topologically the magnetic fluxtubes will reconnect like orthogonal vortex tubes [20] so that two initially straight orthogonal tubes exchange halves to form two tubes bent at right-angles.

In contrast to this picture, we find that for low twist reconnection between the fluxtubes is not substantial, even for low Lundquist numbers. The evolution is primarily an elastic collision of the fluxtubes with little energy released to the plasma. This result is important to models of solar activity, because coronal fluxtubes are believed to have low twist. Our results demonstrate that, at least for modest collision velocities, fluxtube reconnection is much more difficult to accomplish than generally is assumed.

We then attempted to obtain more reconnection by increasing the twist of the fluxtubes to $b = 10$ and by using a low Lundquist number ($S = 576$). Two effects can enhance reconnection for higher twist. First, two null points, at which opposing field lines are exactly anti-parallel, can form in the interaction region. It is widely believed that rapid reconnection is favored at such nulls [21]. Second, as we show below, the reconnected field lines are highly tangled and tend to pull the tubes together, thereby enhancing their interaction. This tangling appears to be the dominant effect. We find that the high-b, low-S case does, indeed, behave like the standard vortex-tube reconnection picture described above [15].

Since low Lundquist numbers generally are not relevant to space plasmas, we then considered the effect of increasing S; our expectation being that, for sufficiently high S, the reconnection rate would decrease to the point that the tubes behave like the low twist case and simply bounce off each other. The actual evolution was a complete surprise — for $S = 2880$ the tubes apparently pass right through each other. This result is demonstrated in Figure 2, which shows isosurfaces of the magnetic field magnitude at six times during the run. The isosurfaces are taken at half the maximum field magnitude value *at each time*. Initially, the horizontal fluxtube is behind the vertical fluxtube. The effect of the first reconnections becomes clear as the reconnected field lines exert a torque on the tubes, giving them a kinked appearance. Later, the singly connected field lines dominate, as the tubes begin to exchange halves. Then the doubly reconnected field dominates, with the central field lines pulling along the rest of the field lines. At the final time, the vertical tube is now in front of the horizontal tube, in contrast with the initial state.

The origin of tunneling can be clarified by close inspection of the magnetic connectivity. Figure 1 shows one winding of two representative field lines before reconnection. Figure 3 shows the effect of the first reconnection, (for clarity only one of the reconnected field lines is shown). Since there are two reconnection regions, each field line tends to reconnect twice. The lines exchange halves to form two right-angle lines, which cannot simply pull away from the reconnection site as in the standard picture, however, because they are wrapped around both fluxtubes. In fact, this tangling tends to pull the tubes together, producing more reconnection. Figure 4 shows the effects of the second reconnection. The vertical field line passes around the horizontal tube, while a similar horizontal field line passes around the vertical tube. Such field lines are now free to continue on their initial trajectory without further interaction. This is the basic mechanism of magnetic tunneling; two reconnections at approximately fixed, diagonally opposite points in the collision region, (see Figure 5), allow vertical and horizontal field lines to exchange central portions and, thereby, pass through each other.

Discussion

Several interesting features and unanswered questions have been raised by our results. First, it is evident from Figure 2 that the post-reconnection fluxtubes have very complex internal structure. In the initial Gold-Hoyle model, all field lines lie on well-defined cylindrical flux surfaces. Some of the initial twist is lost, however, during the double reconnection process — at least one winding. For high S, magnetic helicity is expected to be approximately conserved [22]; hence, the helicity in the twist is transferred to internal wrappings of the field lines about each other. The conclusion is that, as in the case of 2.5D studies [23], reconnection tends to produce a chaotic final field topology. These results imply that magnetic fluxtubes which erupt through the solar surface also are likely to have a complex fine-scale internal structure.

One fascinating aspect of tunneling is the process by which the central field lines near the tube axis pass through each other. The double reconnection mechanism described above should be inapplicable to them since these field lines have vanishing twist. In fact, they also undergo a double reconnection similar to the highly twisted lines. Figure 2 shows that, during the height of the reconnection phase, both fluxtubes are deformed so that they run diagonally through the reconnection sites. We believe that this deformation is due to field lines, such as those in Figure 4, which have already tunneled and exert a torque on the remaining field, causing the central field lines to become parallel in the interaction region. An additional force pulls the axis field lines out of their respective vertical planes and toward the two reconnection sites where they also reconnect and exchange central portions, as seen in Figure 5. The origin of this force is unclear to us, at present. We also do not know whether the observed evolution reflects some general physical property of magnetic fluxtubes or is simply a peculiarity of the system under consideration. It should be noted that, for the high twist case, the energy in the azimuthal field, $2\pi \int {B_\phi}^2\, r dr$, is over 3 times the axial field energy. This is another reason for expecting tunneling to require a large twist. Unless the twist component dominates, it cannot deform the axial component sufficiently for that component to also undergo double reconnection. A further possibly important point is that high twist fluxtubes are expected to be kink unstable. Since the Gold-Hoyle model is metastable to first order, the kink mode growth rate is small, [24]but it may be contributing to the deformation of the axial field.

In the context of solar and space plasmas, the key question is the range of applicability of our results to the very large Lundquist number regime. We have two main conclusions – for modest collision velocities, low twist orthogonal tubes bounce and high twist tubes tunnel. The first result should be even more valid at higher S; hence, fluxtube reconnection is unlikely to be common in the solar corona unless the tubes are driven together, or are nearly anti-parallel. We believe that the second result also holds for higher S because the rate of reconnection depends very weakly on S, but this is only a conjecture. We are currently exploring these issues.

Acknowledgments. We thank Drs. A. B. Hassam and E. R. Priest for helpful conversations. We also thank Drs. J. T. Karpen and J. A. Klimchuk for commenting on the manuscript. This work was sponsored by the NASA High Performance Computing and Communication Program, the NASA Space Physics Theory Program, and ONR. The computations were performed on the Naval Research Laboratory CM5E under a grant of time from the DoD HPC program.

References

1. E. N. Frazier and J. O. Stenflo, Solar Phys. **27**, 330 (1972).

2. P. A. Sturrock and Y. Uchida, Astrophys. J. **246**, 331 (1981).

3. J. T. Karpen, S. K. Antiochos, R. B. Dahlburg and D. S. Spicer, Astrophys. J. **403**,

769 (1993).

4. E. N. Parker, Astrophys. J. **264**, 642 (1983).

5. E. N. Parker, Astrophys. J. **330**, 474 (1988).

6. G. Roumeliotis, Astrophys. J. **379**, 392 (1991).

7. P. A. Sturrock, P. Kaufman, R. L. Moore, and D. F. Smith, Solar Phys. **94**, 341 (1984).

8. M. E. Machado, K. K. Ong, A. G. Emslie, G. Fishman, C. Meegan, R. B. Wilson, and W. S. Paciesas, Adv. Space Res. **13**, 175 (1993).

9. E. G. Zweibel and J. E. Rhoads, Astrophys. J. **440**, 407 (1995).

10. L. W. Klein and L. F. Burlaga, J. Geophys. Res. **87**, 613 (1982).

11. B. U. O. Sonnerup et al., J. Geophys. Res. **86**, 10049 (1981).

12. J. Birn and E. W. Hones, Jr., J. Geophys. Res. **86**, 6802 (1981).

13. R. B. Dahlburg and J. M. Picone, Phys. Fluids B **1**, 2153 (1989).

14. R. B. Dahlburg and S. K. Antiochos, J. Geophys. Res. **100**, 16991 (1995).

15. R. B. Dahlburg and D. Norton, in *Small Scale Structures in Three Dimensional Hydro and Magnetohydrodynamic Turbulence*, eds. M. Meneguzzi, A. Pouquet, and P. -L. Sulem, (Springer-Verlag, Heidelberg, 1995), p. 331.

16. T. Gold and F. Hoyle, M. N. R. A. S. **120**, 89 (1958).

17. C. Canuto, M. Y. Hussaini, A. Quarteroni, and T. A. Zang, *Spectral Methods in Fluid Mechnics*, Springer-Verlag, New York (1987).

18. M. Jardine, J. Plasma Phys. **51**, 399 (1994).

19. T. N. LaRosa and R. L. Moore, Astrophys. J. **418**, 912 (1993).

20. O. N. Boratav, R. B. Pelz, and N. J. Zabusky, Phys. Fluids A **4**, 581 (1992).

21. J. M. Greene, J. Geophys. Res. **93**, 8583 (1988).

22. J. B. Taylor, Phys. Rev. Lett. **33**, 11398 (1974).

23. J. T. Karpen, S. K. Antiochos, and C. R. DeVore, Astrophys. J. Lett., submitted (1995).

24. M. G. Linton, D. W. Longcope, and G. H. Fisher, Astrophys. J., submitted (1995).

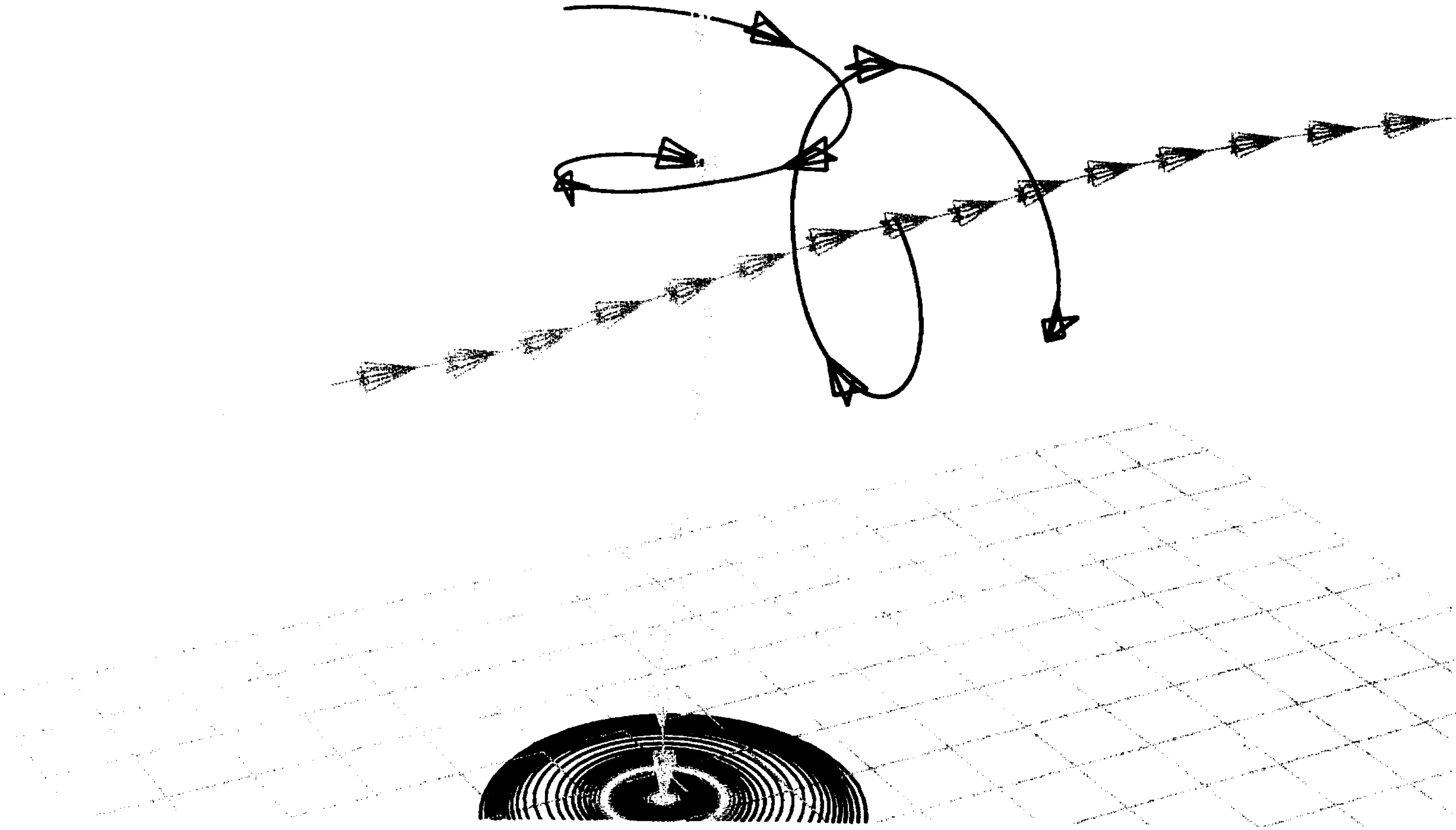

FIGURE 1. Magnetic field lines at $t = 7.8$. Contours of $|\mathbf{B}|$ are shown on the bottom grid in order to indicate the size of the fluxtube. Only every 8th grid line is plotted. The heavily arrowed magnetic field lines pass through the center of the flux tubes. Note that from this viewpoint the vertical central line is behind the horizontal one. Also shown is one winding of a twisted field line near the boundary of each flux tube; red corresponds to the vertical tube and blue to the horizontal tube.

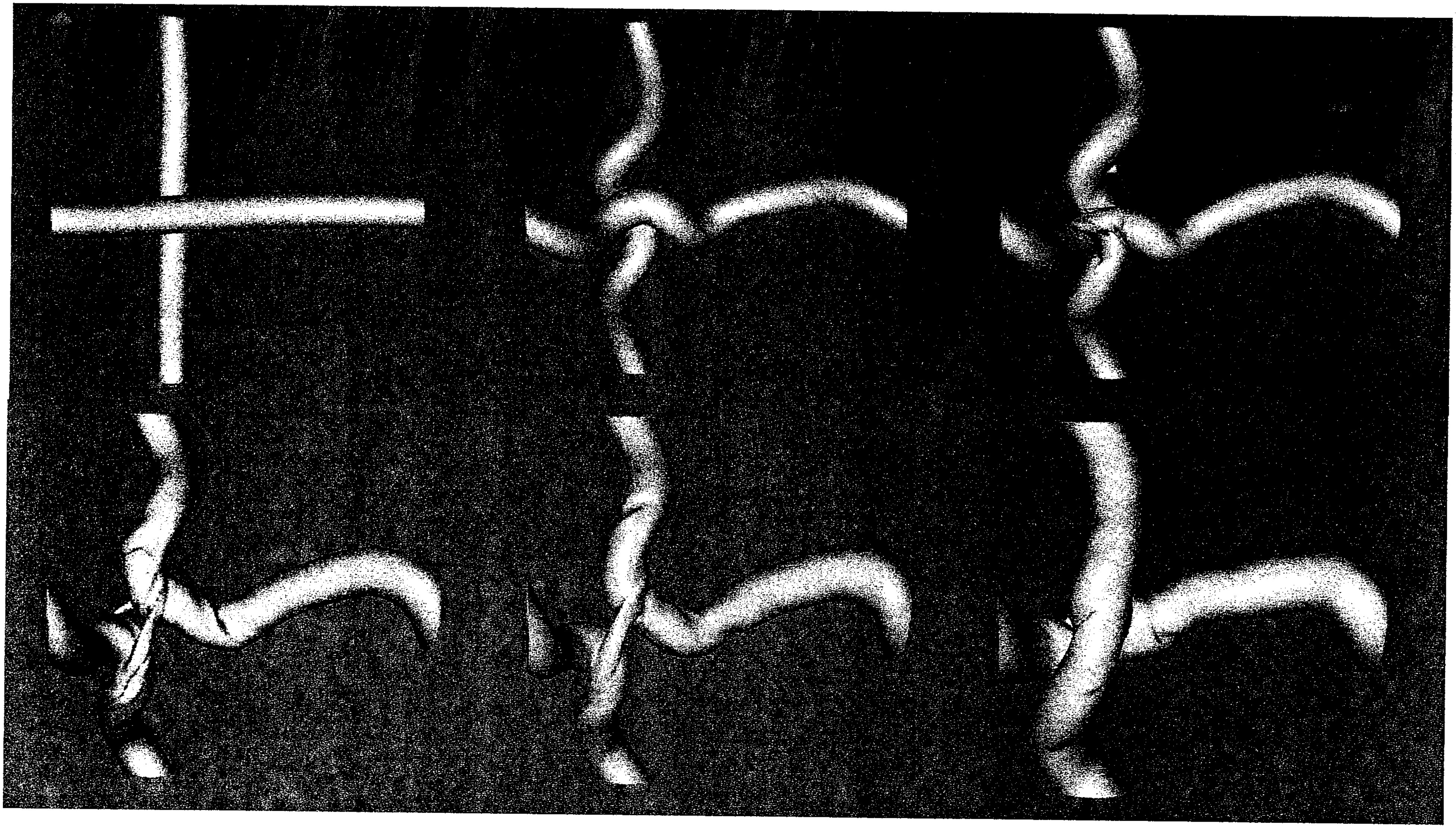

FIGURE 2. Isosurfaces of $|\mathbf{B}|$ at several times during the run. The upper left corner shows the result for $t = 7.8$. To the right are the results for $t = 21.1$ and 30.6. The lower left corner shows the result for $t = 40.8$. To its right are the results for $t = 52.2$ and 64.2. The isosurfaces are chosen to equal $\frac{1}{2}|\mathbf{B}|_{max}$ at each time.

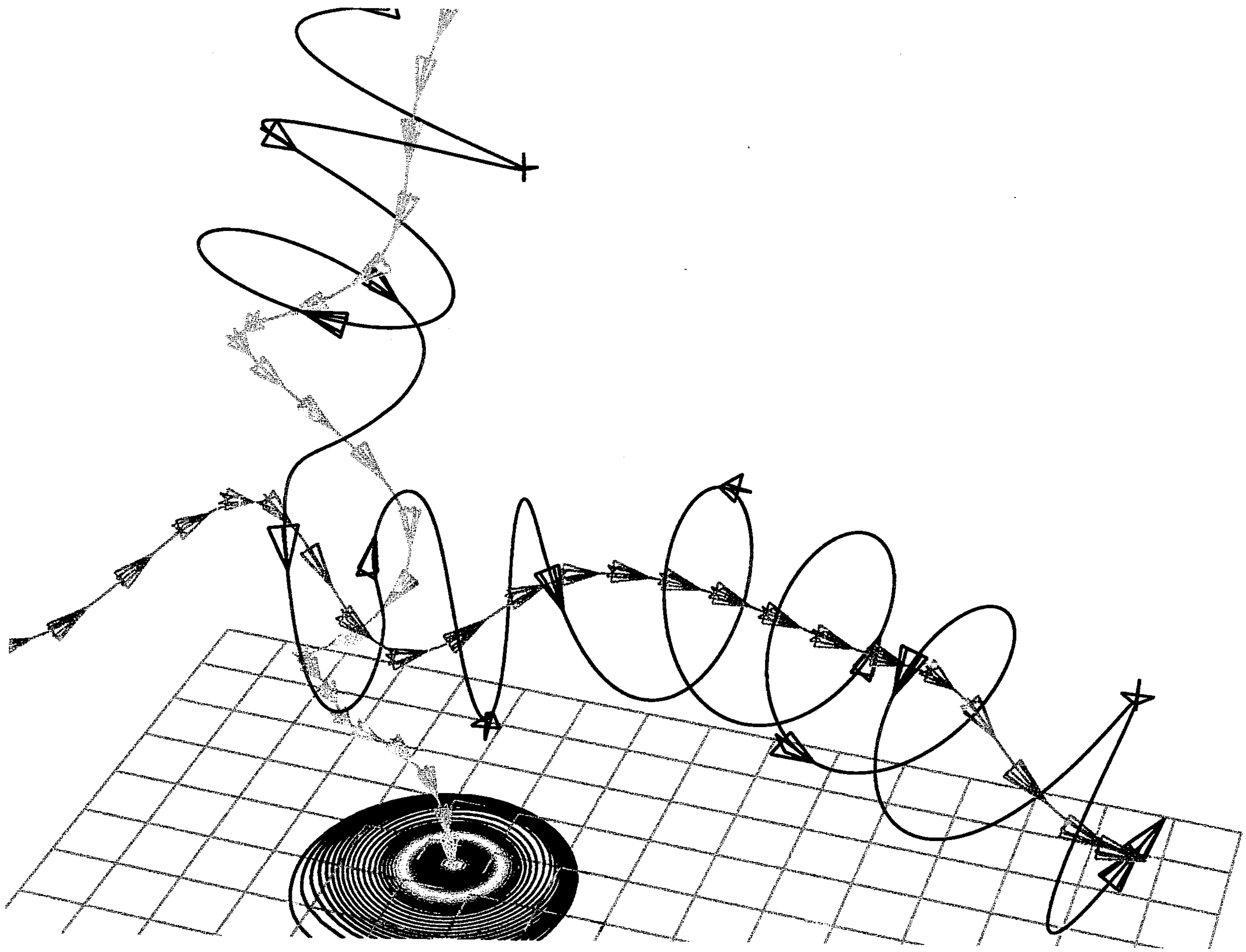

FIGURE 3. A reconnected field line at $t = 16.6$. The contours, grid and heavily arrowed lines are as in Figure 1, and the viewpoint is very similar; there has been a small clockwise rotation about the vertical axis. Note that the red field line begins as a vertical twisted line, but then bends to become a horizontal line.

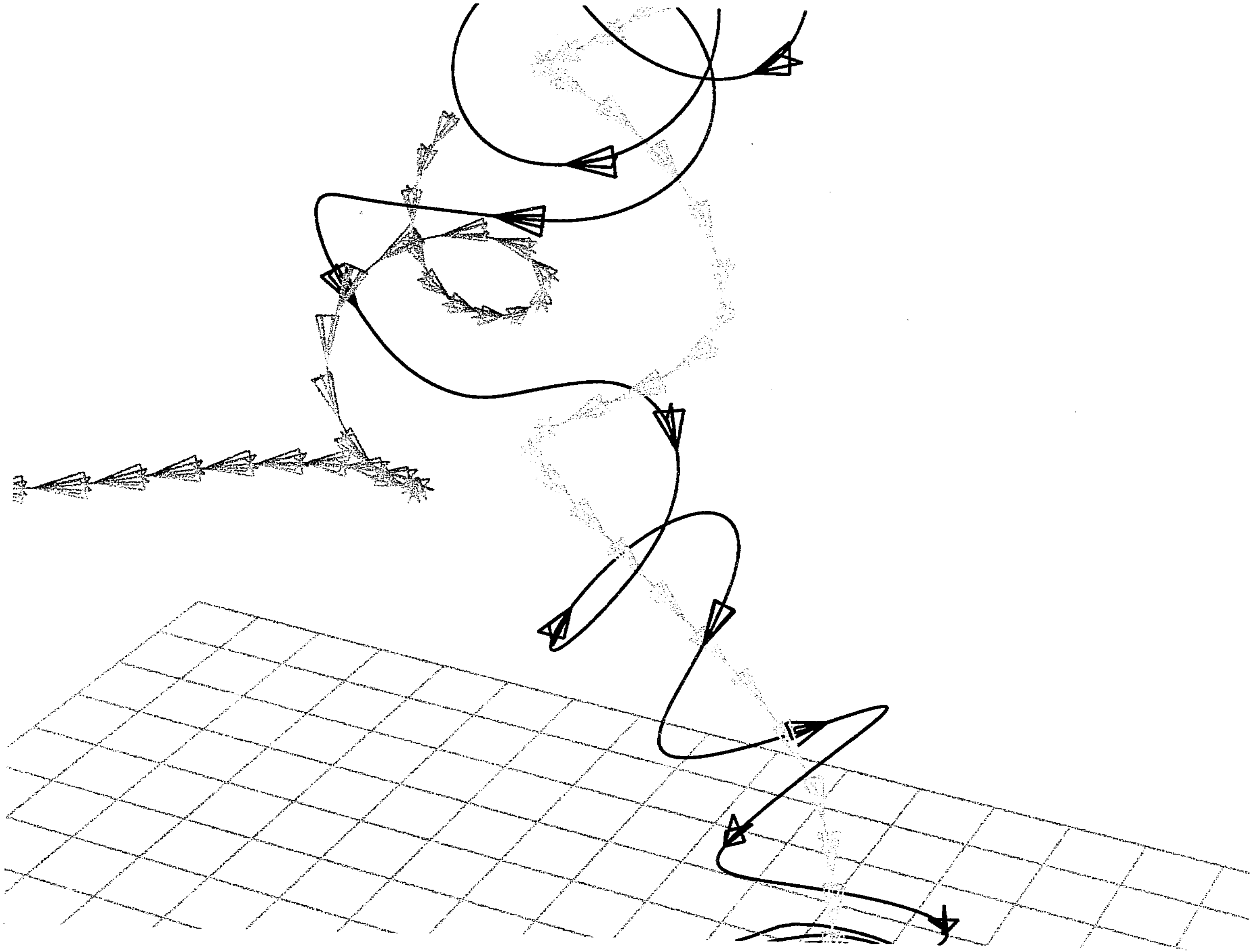

FIGURE 4. A doubly reconnected field line at $t = 21.1$. The contours, grid, and heavily arrowed lines are as in Figure 3, but for clarity the viewpoint has been rotated clockwise by roughly $\pi/2$ so that the right grid corner in this Figure corresponds to the left corner visible in Figure 3. Note that the red field line begins and ends as a vertical twisted line, but also wraps around the horizontal central line.

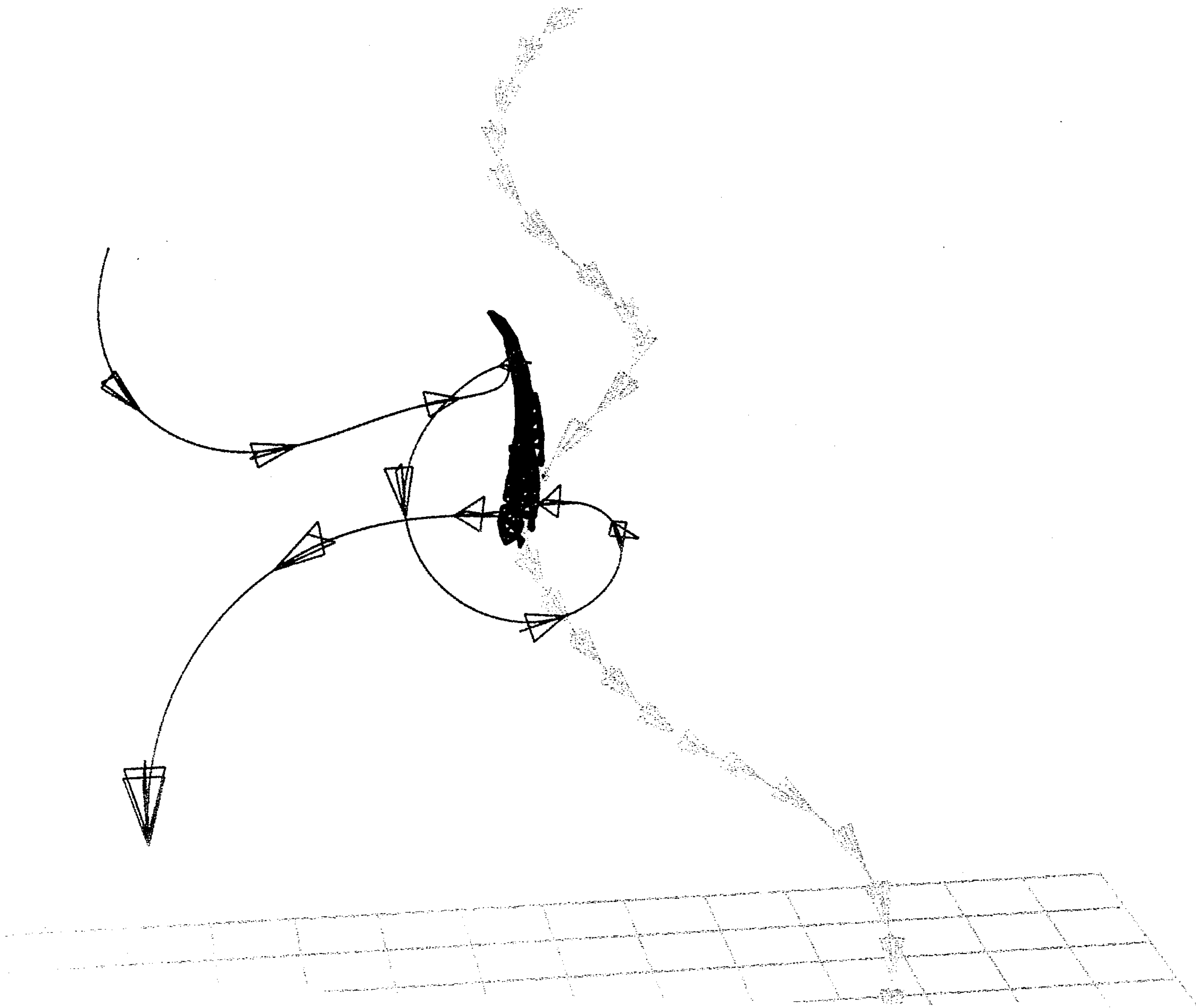

FIGURE 5. A view of the central magnetic field lines at $t = 30.6$, showing that the horizontal field line is pulled at two locations toward the vertical field line. Reconnection at these locations will allow the horizontal line to pass around the vertical one. The contours, grid and heavily arrowed lines are as in Figure 4, and the viewpoint is very similar, except for a small counterclockwise rotation. Also shown in red is the electric current magnitude isosurface at 75% of maximum. Note that this surface resembles a sheet lying diagonally between the colliding magnetic field lines.